VU VRIJE UNIVERSITEIT AMSTERDAM

VU Research Portal

(pi^{andplusmn;},2N) reactions at 165 and 245 MeV

Altman, A.; Ashery, D.; Bertl, W.; Felawka, L.; Lichtenstadt, J.; Piasetzky, E.; Pluym, J. v. d.; Powers, R.J.; Walter, H.K.; Winter, R.G.; Yavin, A.I.

published in
Default journal
1986

document version
Publisher's PDF, also known as Version of record

Link to publication in VU Research Portal

citation for published version (APA)
Altman, A., Ashery, D., Bertl, W., Felawka, L., Lichtenstadt, J., Piasetzky, E., Pluym, J. V. D., Powers, R. J., Walter, H. K., Winter, R. G., & Yavin, A. I. (1986). (pi^{andplusmn;},2N) reactions at 165 and 245 MeV. *Default journal*.

General rights
Copyright and moral rights for the publications made accessible in the public portal are retained by the authors and/or other copyright owners and it is a condition of accessing publications that users recognise and abide by the legal requirements associated with these rights.

- Users may download and print one copy of any publication from the public portal for the purpose of private study or research.
- You may not further distribute the material or use it for any profit-making activity or commercial gain
- You may freely distribute the URL identifying the publication in the public portal

Take down policy
If you believe that this document breaches copyright please contact us providing details, and we will remove access to the work immediately and investigate your claim.

E-mail address:
vuresearchportal.ub@vu.nl

Download date: 28. Mar. 2024

$(\pi^{\pm},2N)$ reactions at 165 and 245 MeV

A. Altman,* D. Ashery, E. Piasetzky, J. Lichtenstadt, and A. I. Yavin
Raymond and Beverly Sackler Faculty of Exact Sciences, School of Physics and Astronomy, Tel-Aviv University, Tel-Aviv, Israel

W. Bertl, L. Felawka,* and H. K. Walter
Institut für Mittelenergiephysik der Eidgenössische Technische Hochschule Zürich, CH-5234 Villigen, Switzerland

R. J. Powers†
Physikinstitut der Universität Zürich, CH-8001 Zürich, Switzerland

R. G. Winter
Universität Zürich, CH-8001 Zürich, Switzerland and College of William and Mary, Williamsburg, Virginia

J. v. d. Pluym
Naturkundig Laboratorium, Vrije Universiteit, Amsterdam, The Netherlands

(Received 9 December 1985)

The $(\pi^+,2p)$ and $(\pi^{\pm}, pn)$ reactions were studied by coincidence detection of the outgoing nucleons on C, Fe, and Bi at 165 and 245 MeV and on ^{16}O and ^{18}O at 165 MeV. The quasideuteron component is identified and found to account for only about 10% of the absorption cross section for carbon down to about 2% for bismuth. With corrections for the final-state interaction of outgoing nucleons it amounts to at most 40%. The data indicate that quasideuteron absorption following pion scattering is not likely. The absorption on $T=1$ nucleon pairs is about 4% of that on quasideuterons.

I. INTRODUCTION

Pion absorption on a nucleon pair is the simplest mode of pion annihilation in nuclei. The question of whether this is also the dominant mode has created much controversy in recent years. The fact that it has a free counterpart in pion absorption on the deuteron has made the "quasideuteron" model a convenient framework for the theoretical study of pion absorption. Some theoretical calculations[1-3] were able to reproduce reasonably well experimental data of total absorption cross sections, assuming only absorption on nucleon pairs together with the contribution of initial-state interaction of the incoming pion or followed by final-state interaction of the outgoing nucleons. The concept of two-nucleon absorption motivated the setup of a number of experiments aimed specifically to study this mechanism.[4-8] It has also influenced the way in which pion annihilation traditionally enters the pion nucleus potential. At threshold, the imaginary part of the optical potential is assumed to be proportional to the square of the density.[9] In the (3,3) resonance region the interaction between the pion and the nucleus is described through formation of the Δ resonance and one introduces a Δ-nucleus "spreading" potential proportional to the density,[10] which also implies a basic two-nucleon process.

Soon it was realized, however, that pion absorption on complex nuclei displays features which do not reflect in an obvious way the assumed "quasideuteron" mechanism. Already in a bubble chamber experiment of Bellotti *et al.*,[11] events where two fast protons escape with essentially all the available energy contributed only a small fraction ($\sim 10\%$) of the total absorption cross section on ^{12}C at 130 MeV. In most cases the energy is distributed among more nucleons or heavier fragments. The conclusion of this early work was that capture on an α-like "cluster" plays an important role in pion absorption. Later, coincidence experiments by the authors of the present work[12] of the $(\pi^+,2p)$ reaction on and above the (3,3) resonance on ^{12}C showed the same features, namely a contribution of about 10% to the total absorption cross section. The total two-nucleon absorption cross section with two fast outgoing protons may be larger if final-state interaction of the outgoing nucleons is considered.

Inclusive single-arm measurements of proton spectra following pion interaction with nuclei[13] show a high energy peak, characteristic of the absorption on a nucleon pair, only for very light nuclei and at forward angles. It has been suggested that more complicated processes take part in the absorption reaction; based on rapidity analysis of single-arm proton spectra, it was concluded that on the average about four nucleons are involved. Furthermore, the ratio R of proton yields, following π^+ and π^- interaction, $R \equiv Y_p(\pi^+)/Y_p(\pi^-)$, is found to be around 4, whereas the "quasideuteron" absorption through a ΔN intermediate state would suggest a ratio larger than 10. More exclusive pion absorption experiments probing the two-body mechanism on light nuclei[14] show that the ratio R is indeed large and about 1 order of magnitude larger than expected from inclusive data. A series of coincidence measurements to study the $(\pi,2N)$ reaction on ^3He has been performed at resonance energy at LAMPF (Ref. 15) and SIN (Ref. 16) and at low energy at TRIUMF

 ©1986 The American Physical Society

(Ref. 17). All these experiments show a ratio

$$R \equiv \sigma^3\mathrm{He}(\pi^+,2\mathrm{p})/\sigma^3\mathrm{He}(\pi^-,\mathrm{pn})$$

between 15 at low energy and 35 at the Δ-resonance energy. These ratios are much larger than those observed in the inclusive single-arm data.

Secondary interactions such as final-state interaction and rescattering of the two outgoing nucleons following absorption by a nucleon pair do not supply a satisfactory explanation for all the observations mentioned above, for two reasons. First, the mean free path of ~100 MeV nucleons in nuclear matter is large, typically 5 fm;[13] therefore, very large rescattering effects are unlikely—especially in very light nuclei. Second, the velocity distributions of protons coming from π^+ and π^- absorption on medium to heavy nuclei are very similar.[13] This behavior would be hard to understand if initial two-body processes together with secondary interactions were important, since the protons in the π^+ absorption can result from primary and secondary interactions, whereas most of the protons from the π^- absorption must be secondary ones.[13] Transport calculations,[18] which invoke a considerable amount of pion scattering—including charge exchange—prior to absorption, can partly reproduce the results of the rapidity analysis.

The purpose of this work was to shed more light on the problems discussed above. We report results on the cross sections of the $(\pi^+,2\mathrm{p})$ and $(\pi^\pm,\mathrm{pn})$ reactions on ^{12}C, ^{16}O, ^{18}O, Fe, and Bi at 165 and 245 MeV. Angular correlations of the two outgoing nucleons, as well as differential and integrated cross sections were obtained. We list in Table I the reactions and targets that were investigated, and the incident energies and angular ranges at which these investigations were done.

II. THE EXPERIMENTAL METHOD

The experiment was performed at the $\pi M3$ channel of the SIN accelerator at bombarding energies of 165 and 245 MeV for positive and negative incident pions. The outgoing nucleon pairs were detected in coincidence. Natural targets of C, Fe, and Bi of thickness 2, 2.5, and 4.5 g/cm^2, respectively, were used. For ^{16}O and ^{18}O we used $H_2{}^{16}O$ and $H_2{}^{18}O$ (99.1%) targets. The water was contained in $50\times50\times10$ mm^3 plastic containers with 0.5 mm thick windows while an empty identical box was used for background measurements. The experimental setup is shown in Fig. 1. The pion beam hit the target after passing through two plastic scintillators, P_1 and P_2. The target was fitted into a 5×5 cm^2 hole in the center of a large plastic scintillator P_4. An anticoincidence with this collimating scintillator and a coincidence with the two scintillators P_1 and P_2 were required for beam monitoring and data acquisition. Protons present in the beam were eliminated by degraders positioned inside the beam transport channel. Muon and electron contaminations in the beam were measured by time-of-flight technique.

The protons were detected by three telescopes, each

TABLE I. Targets, incident energies, and angular ranges for which the various reaction modes were studied.

Target nucleus	Reaction	Detected angular range of p_1 (deg)	Detected angular[a] range of p_2 for each p_1 angle (deg)	Incident π energy (MeV)
^{12}C	$(\pi^+,2\mathrm{p})$	50–140	>100	165
		50–140	>100	245
^{16}O	$(\pi^+,2\mathrm{p})$	90–140	>100	165
^{18}O	$(\pi^+,2\mathrm{p})$	90–140	>100	165
Fe	$(\pi^+,2\mathrm{p})$	50–140	>100	165
		50–140	>100	245
Bi	$(\pi^+,2\mathrm{p})$	50–140	>100	165
		50–140	>100	245
^{12}C	(π^-,pn)	120–140	>100	165
		120–140	70	245
^{12}C	(π^+,pn)	120–140	40	165
		120–140	50	245
^{16,18}O	(π^-,pn)	120–140	70	165
	(π^+,pn)	120–140	40	165
Bi	(π^-,pn)	120–140	>100	165
		120–140	70	245
Bi	(π^+,pn)	120–140	40	245

[a]Centered around the angle conjugate to θ_{p_1}.

consisting of two $5\times5\times5$ cm^3 cubes of plastic scintillators with 5 mm thick scintillators in front and back of the cubes (the back detector is not shown in the figure). The front surface of the telescopes was 50 cm from the target and their centers separated from each other by 10°. Fast protons that passed through the front counter of a telescope were identified by the combination of their energy losses ($\Delta E1$, $\Delta E2$) in the two scintillators. Particles that passed through both counters were tagged by the scintillator positioned behind the telescopes (not shown in Fig. 1). Slow protons that stopped in the front counter were identified by the combination of their energy losses (ΔE_0, $\Delta E1$) in the front thin detector and in the first thick scintillator. The energy loss measurements, therefore, identified protons over the whole energy region above a threshold of 30 MeV. The proton energy spectrum in the telescopes was not measured. The nucleons, in coincidence with protons in the telescopes, were detected with an array of twenty $5\times100\times10$ cm^3 plastic scintillator bars, arranged in two layers covering an area of 1 m^2 and a total thickness of 10 cm. The front surface of the first layer was 111 cm from the target (Fig. 1). The array could be moved so that the angular range between $-140°$ and 30° relative to the beam direction could be covered continuously. The vertical angular range from $-20°$ to 20° was covered simultaneously. A 1 mm thick scintillator was placed in front of the array to separate neutrons from protons. Pulse height and time-of-flight information was recorded for each scintillator in the array. The time difference between pulses in the phototubes mounted at the ends of each scintillator was used to define the vertical position of the detected particle. The information was sufficient to identify protons and neutrons and to measure their energy (using the time-of-flight information) with moderate resolution. Fast protons that passed through one of the front bars were identified by combining their energy losses in the front and back bars. Particles which stopped in one of the front bars were identified by their position in the energy versus time-of-flight spectrum. Neutrons were identified by lack of signal in the thin scintillator in front of the array and by their position in the energy versus time-of-flight spectrum. This method enabled the separation of neutrons from γ events as illustrated in Fig. 2. The neutron detection efficiency was calculated with a code originally written by Kurz[19] and modified at the University of Karlsruhe.[20] The code reproduced well previously measured neutron detection efficiencies of the same array.[21]

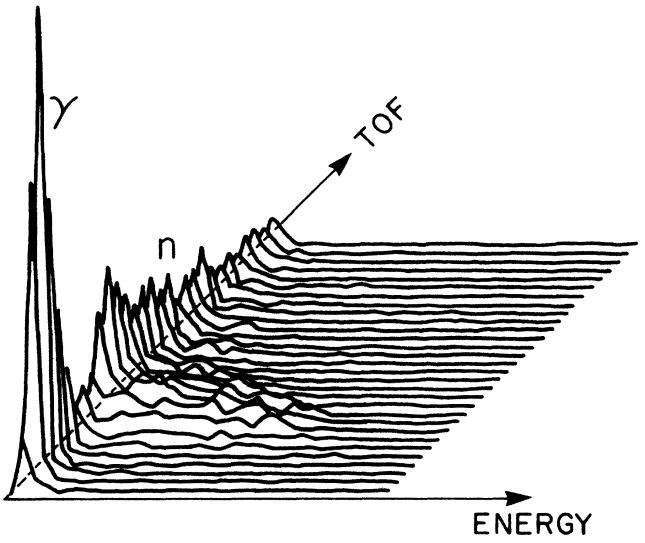


FIG. 2. Time of flight vs energy spectrum for neutral particles in the detector array.

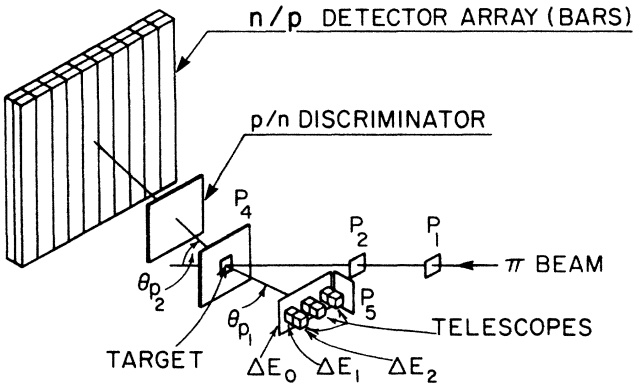


FIG. 1. Experimental setup.

Protons from pion absorption on the deuteron in a D_2O target and protons from pion scattering on the hydrogen in a CH_2 target were detected in coincidence at several angles to provide proton energy calibration in the bars. The overall energy resolution measured with the D_2O target (including kinematic broadening, energy losses, and electronics) was 30 MeV for protons of 200 MeV. The $\pi^+p\rightarrow\pi^+p$ and $\pi^+d\rightarrow pp$ reactions were used also for absolute normalization by using previously measured cross sections.[22,23] The angular resolution for nucleons detected in the array was 5° in the horizontal (reaction) plane and 4° in the vertical plane.

For each position of the proton-detector array, the target angle was fixed so that the proton path in the target was minimized. Corrections were applied to account for loss of protons and neutrons in the target due to secondary reactions as well as to the stopping of low energy protons in the target and the air. The combined muon and electron contamination was 0.5% and 4% for π^+, and 2% and 7% for π^- at 245 and 165 MeV, respectively. All these corrections were included in the absolute normalization.

III. THE π^+,2p REACTION

A. Results

For the study of the (π^+,2p) reactions angular correlations were measured at nine positions. The protons in the telescopes were detected in the angular range of 50°—140° in steps of 10° (excluding the position at 80°). For each such detection angle, protons in the array were detected over an angular range of about 100°, centered around the angle of the $\pi^+d\rightarrow pp$ kinematics, and covering simultaneously a vertical angular range $-20°<\phi<20°$. A

three-dimensional display of the proton-proton angular correlation, integrated over the particle energies, is shown in Fig. 3 for protons in the telescope detected at 140° and for incident kinetic energy of 245 MeV. A pronounced peak is observed at the angle corresponding to the kinematic condition of the $\pi^+ d \rightarrow pp$ reaction superimposed on a "background." Figure 4 shows a slice of this correlation along the reaction plane, with a vertical width $\Delta\phi \pm 6°$, for ^{12}C, ^{16}O, ^{18}O, Fe, and Bi at 165 MeV. The data are integrated over the outgoing proton energies above a cutoff set 80–100 MeV below the peak of their energy spectrum (e.g., Fig. 5). The angular correlation in the vertical plane was found to have a similar shape. This is illustrated in Fig. 6, where we display a cut through the data in the vertical plane together with the data and the fit (see below) done for the horizontal (reaction) plane. The result indicates that the spatial distribution of the observed peak is approximately symmetric in all dimensions about its center.

The errors shown in the figures contain statistical and angle-dependent systematic uncertainties. There is an additional overall normalization uncertainty of 9%.

Each p-p angular correlation was fitted by a least-squares method to a sum of two two-dimensional Gaussian functions (the solid curve in Fig. 4). The peak positions, amplitudes, and widths of these functions were treated as free parameters. We obtained, for all cases, one narrow and one broad Gaussian. The peak of the narrow Gaussian was always found to be very near the angle corresponding to the $\pi^+ d \rightarrow pp$ kinematics. These results suggest the identification of the narrow Gaussian component in the angular correlation with a direct absorption on a p-n pair. This may exclude processes in which the pion scattered (on the energy shell) before absorption or the outgoing protons interacted in the nucleus before emerging. The broad Gaussian (the dashed curve in Fig. 4) is attributed to a background generated by a final-state interaction on the outgoing protons, initial-state interaction

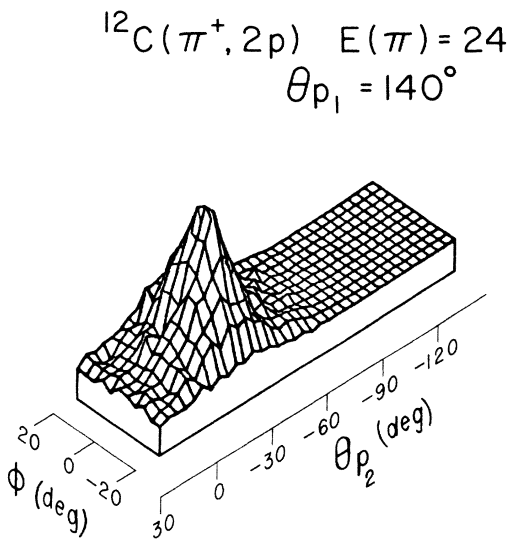


FIG. 3. Three-dimensional display of a proton-proton angular correlation.

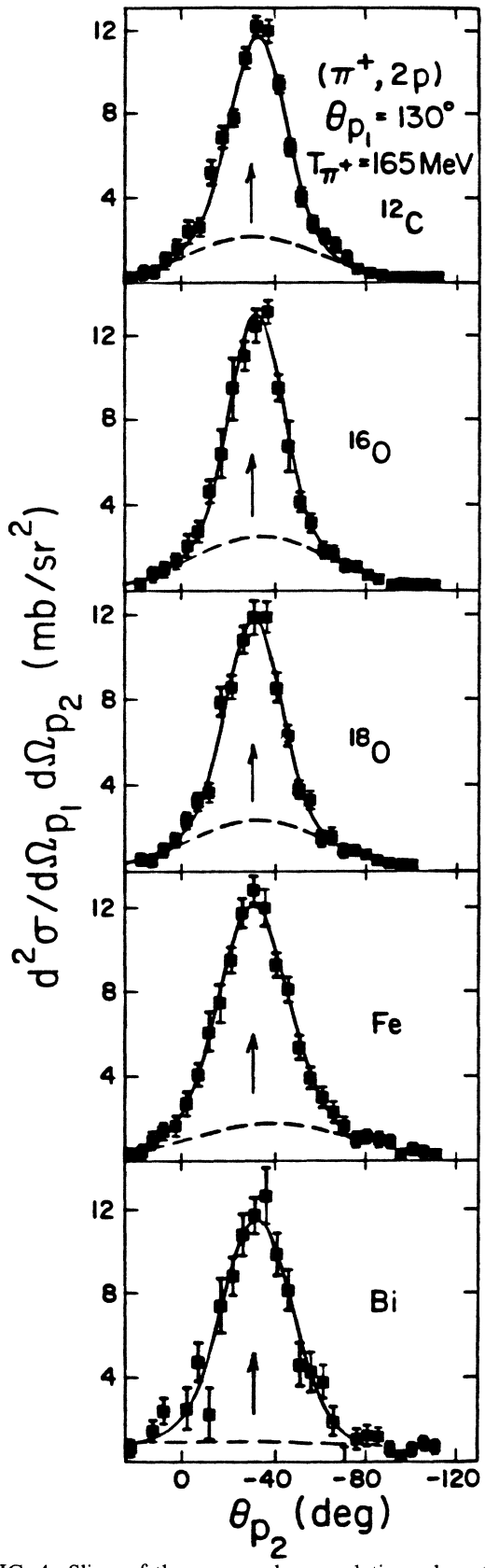


FIG. 4. Slices of the p-p angular correlations along the reaction plane with vertical width of $\Delta\phi = \pm 6°$ for C, ^{16}O, ^{18}O, Fe, and Bi. The solid curves are results of two-Gaussian fits to the data. Dashed curves are the broad Gaussian background. The arrows mark the angle for the $\pi^+ d \rightarrow pp$ reaction

of the incoming pion, and perhaps by more complex absorption mechanisms. The broad Gaussian may also contain some amount of absorption on quasideuterons which are in $l \neq 0$ with respect to the core, as recently suggested by Ritchie *et al.*[24] This contribution should be, however, small, as shown by the distorted-wave impulse approximation (DWIA) calculations of Ref. 24. A further analysis of the broad Gaussian is not pursued in this work for the following reasons: (1) Unlike the narrow Gaussian, the magnitude and shape of the broad Gaussian are sensitive to the energy cutoff which is applied. (2) It is not clear that a Gaussian form is justified for the purpose of extrapolation into the unmeasured part of the phase space. (3) Proton multiplicity of more than 2 may contribute to this component. We therefore concentrate on understanding the properties and physical significance of the narrow Gaussian. In Table II we present the parameters of the narrow Gaussian function resulting from the fit described above.

We examined our results to determine whether a p (pn) component[12] could be included in our p-p quasideuteron results. In this kinematical case a proton and a neutron are going out in the same direction as if they are a single particle in coincidence with another proton. Such a component yields proton energies 40 MeV higher than those from quasideuteron absorption and should be seen as a peak at the higher part of the proton spectrum (e.g., Fig. 5). No such peak was observed but the data cannot rule out a small contribution from this process.

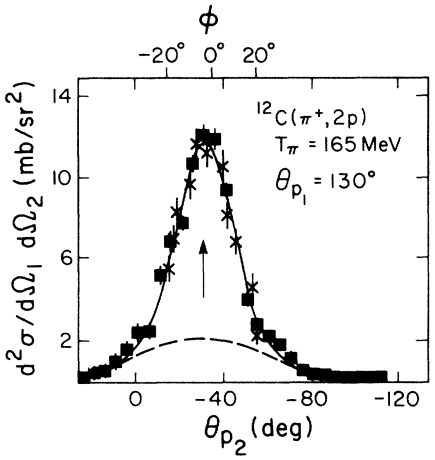


FIG. 6. A slice ($\Delta\theta = \pm 5°$) of the C(π^+,2p) angular correlation in a plane perpendicular to the reaction plane (crosses) together with a similar slice ($\Delta\phi = \pm 6°$) in the reaction plane (squares). The solid and dashed curves have the same meaning as in Fig. 4.

B. Discussion

1. The shape of the angular correlation

The width of the narrow Gaussian is expected to be determined by the momentum of the outgoing proton and that of the absorbing pair with respect to the rest of the nucleus. In an impulse model, if σ is the standard devia-

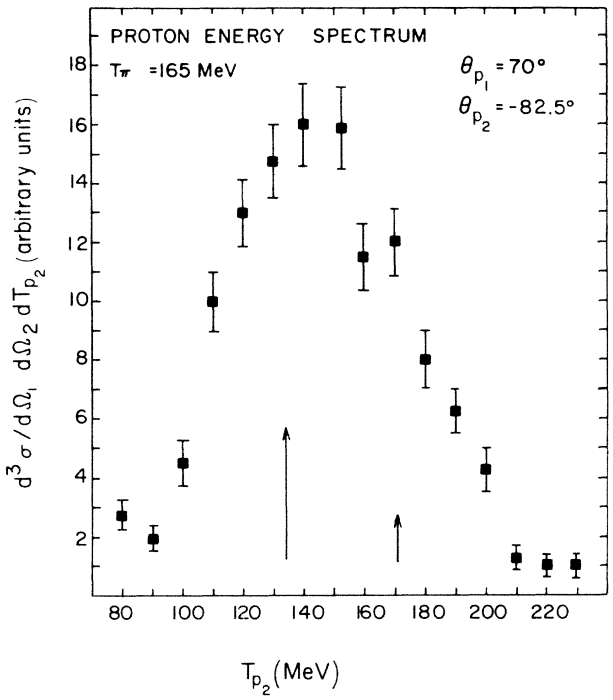


FIG. 5. Proton energy spectrum from the ^{12}C(π^+,2p) reaction measured at $-82.5°$ in coincidence with protons detected at 70°. The long arrow marks the proton energy for the $\pi^+ + {}^{12}\text{C} \rightarrow 2\text{p} + {}^{10}\text{B}$ g.s. The short arrow marks the proton energy for the $\pi^+ + {}^{12}\text{C} \rightarrow \text{p} + (\text{pn}) + {}^{9}\text{B}$. In both cases the residual nucleus is assumed to be at rest.

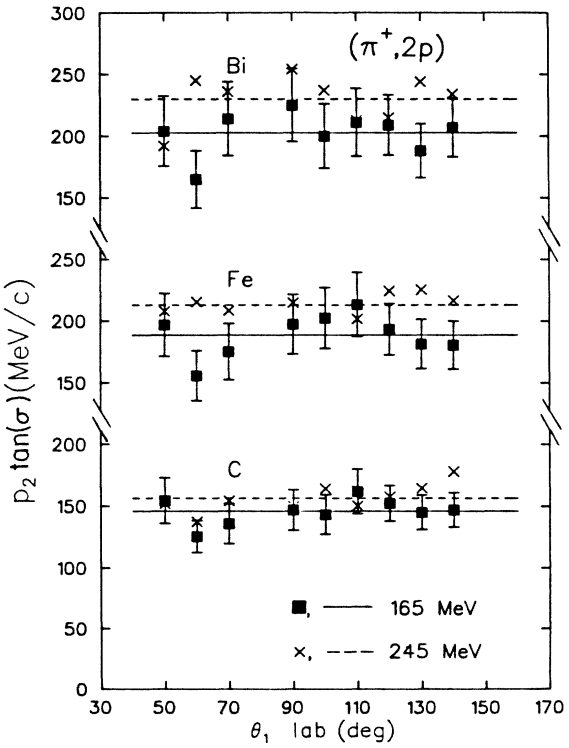


FIG. 7. $p_2\tan(\sigma)$ vs θ_1 lab; the solid and dashed lines represent the average P_{qd} values for 165 and 245 MeV, respectively. (See text for definitions of p_2, P_{qd}, and σ.)

TABLE II. The parameters of the narrow Gaussian (quasi-deuteron), the angle for the free $\pi^+ d \rightarrow 2p$ reaction and the integration of the narrow Gaussian over θ_2, namely the differential cross section for the $(\pi^+,2p)$ reaction. The errors are only statistical. The results are presented for 165 and 245 MeV.

		Parameters of the quasideuteron Gaussian				
	θ_{p_1} lab (deg)	Amplitude (mb/sr^2)	Standard deviation (deg)	Peak angle (deg)	p_2 angle from $\pi d \rightarrow 2p$ kinematics (deg)	$d\sigma/d\Omega_{p_1}$ lab (mb/sr)
			$T_\pi = 165$ MeV			
C	50	5.48	17.1	104.2	105	3.06±0.40
	60	5.36	13.6	92.7	93	1.90±0.30
	70	3.99	14.0	83.4	82	1.50±0.23
	90	3.88	13.9	60.7	62	1.43±0.23
	100	5.90	13.1	53.7	54	1.93±0.27
	110	6.59	14.4	45.5	46	2.62±0.36
	120	8.10	13.3	37.2	39	2.74±0.37
	130	9.51	12.4	31.3	31	2.79±0.34
	140	7.98	12.4	23.3	25	2.33±0.46
^{16}O	90	6.29	13.8	62.1	62	2.30±0.36
	100	6.15	13.5	53.2	54	2.14±0.27
	110	8.49	13.6	43.8	46	2.98±0.42
	120	9.71	12.4	36.3	39	2.85±0.37
	130	10.43	11.8	30.9	31	2.77±0.34
	140	10.56	12.0	23.4	25	2.89±0.35
^{18}O	90	7.52	13.2	58.6	62	2.50±0.35
	100	7.40	12.5	53.0	54	2.22±0.20
	110	9.31	13.6	44.2	46	3.31±0.41
	120	9.20	12.9	36.1	39	2.93±0.37
	130	9.37	12.3	30.3	31	2.72±0.34
	140	10.73	12.2	22.7	25	3.05±0.36
Fe	50	4.83	21.4	105.5	105	4.22±0.81
	60	5.16	16.7	93.2	93	2.74±0.57
	70	4.00	17.8	82.0	82	2.51±0.44
	90	3.69	18.4	64.4	62	2.40±0.38
	100	6.45	18.2	51.8	54	4.09±0.52
	110	6.68	18.7	42.2	46	4.45±0.54
	120	8.65	16.7	35.6	39	4.60±0.49
	130	10.37	15.4	30.2	31	4.67±0.51
	140	9.35	15.1	24.6	25	4.10±0.48
Bi	50	4.51	22.1	108.4	105	4.20±0.71
	60	4.43	17.6	94.7	93	2.63±0.50
	70	3.06	21.4	82.5	82	2.69±0.50
	90	3.71	20.8	64.9	62	3.07±0.50
	100	5.66	18.0	53.7	54	3.51±0.57
	110	6.13	18.5	46.7	46	4.01±0.65
	120	8.76	17.8	38.7	39	5.41±0.74
	130	10.53	15.9	31.8	31	5.11±0.65
	140	10.40	15.0	25.5	25	4.49±0.61
			$T_\pi = 245$ MeV			
C	50	3.81	15.5	101.0	100	1.74±0.28
	60	2.98	13.2	87.3	88	1.00±0.17
	70	2.01	14.0	74.2	77	0.76±0.12
	90	3.79	12.4	55.4	58	1.11±0.32
	100	4.69	13.1	48.4	50	1.55±0.24
	110	5.58	11.6	42.5	42	1.42±0.19
	120	6.02	11.9	34.7	35	1.61±0.21
	130	6.09	12.3	28.4	29	1.75±0.22
	140	5.59	13.0	21.4	23	1.81±0.24

TABLE II. (*Continued*).

	θ_{p_1} lab (deg)	Parameters of the quasideuteron Gaussian Amplitude (mb/sr^2)	Standard deviation (deg)	Peak angle (deg)	p_2 angle from πd→2p kinematics (deg)	$d\sigma/d\Omega_{p_1}$ lab (mb/sr)
Fe	50	3.90	20.8	109.0	100	3.22±0.56
	60	3.50	20.2	87.9	88	2.73±0.46
	70	3.33	18.6	76.3	77	2.19±0.35
	90	4.57	17.5	54.4	58	2.66±0.46
	100	5.72	16.0	48.7	50	2.81±0.42
	110	6.89	15.4	39.3	42	3.13±0.47
	120	7.50	16.7	33.9	35	4.00±0.51
	130	7.87	16.5	27.6	29	4.11±0.54
	140	6.47	15.7	23.4	23	3.05±0.42
Bi	50	4.84	19.3	102.8	100	3.45±0.63
	60	3.65	22.7	90.2	88	3.59±0.64
	70	3.14	20.9	78.5	77	2.61±0.41
	90	4.16	20.5	55.0	58	3.33±0.50
	100	5.66	18.6	45.7	50	3.73±0.55
	110	6.61	16.3	41.4	42	3.34±0.50
	120	7.92	16.1	35.1	35	3.91±0.52
	130	7.88	17.8	27.7	29	4.77±0.63
	140	7.83	16.9	20.3	23	4.27±0.59

tion of the narrow Gaussian, we may expect $\tan(\sigma) \sim P_{qd}/P_N$, where P_{qd} is the momentum of the absorbing quasideuteron in the nucleus and P_N is the average momentum of the outgoing nucleon for which the angular correlation is measured. In Fig. 7 we plot the values of $P_N\tan(\sigma)$ and indicate the average P_{qd} values by the straight lines. We note that the trend is indeed reproduced by this simple model which, again, reflects a simple one-step mechanism. The values of the momenta for the absorbing pair are of the same order of magnitude as the Fermi momentum. We note that there is a significant increase in P_{qd} between ^{12}C and Fe, but between Fe and Bi the difference is small. These momenta describe nucleons on the surface, where absorption occurs, and therefore reflect a local density. This indeed changes, on the surface, more between ^{12}C and Fe than between Fe and Bi. We also note a small but systematic energy dependence. This may reflect the depth of penetration of the pion, being larger at 245 MeV than at the resonance region of 165 MeV. As a result the average quasideuteron momentum is slightly higher for 245 MeV, representing higher density.

We now examine the symmetry of the angular correlation about the central angle. If we consider the case of $\theta_{p_1}=70°$ ($\equiv 83°$ c.m. for 165 MeV and 86° c.m. for 245 MeV), we note from πd→pp kinematics that at this angle the opening angle between the two outgoing protons is minimal (see Fig. 8). If the pion scattered (on the energy shell) before absorption, θ_{p_1} is no longer 70° with respect to its direction when absorbed. This will result in a larger opening angle. The scattered pion also has lower energy and this, again, increases the opening angle. A significant amount of such initial-state interactions of the pion should manifest itself in an asymmetric angular correlation with more events on the larger opening angle side; a shift of the centroid of the angular correlation towards larger angles would also then occur. Observation of the angular correlation for θ_{p_1} at 70° (Fig. 9) does not show any such asymmetry or shift, within the precision of the present work. For comparison, a prediction of cascade

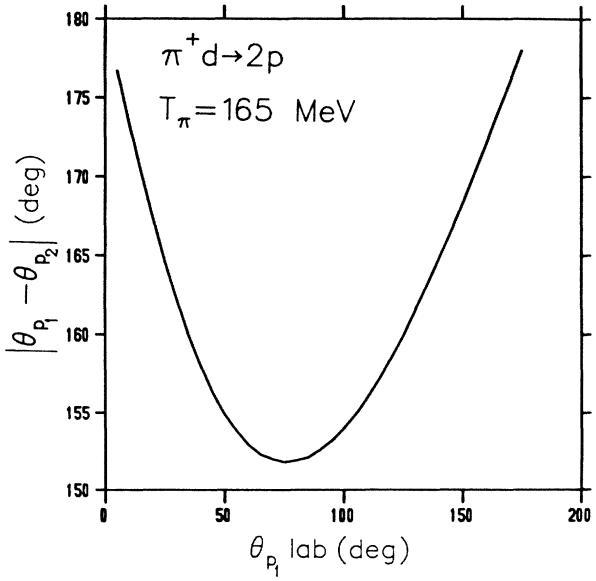


FIG. 8. The opening angle of the two outgoing protons from a π^+d→2p reaction as a function of the angle of one of them for T_π=165 MeV.

calculations for this angular correlation is shown in Fig. 9 by a dashed line and an asymmetry is noticeable. To quantify this effect, we define the asymmetry

$$A=\frac{|\theta_+-\theta_0|-|\theta_--\theta_0|}{|\theta_+-\theta_0|+|\theta_--\theta_0|},$$

where θ_0 is the peak angle, and θ_+ and θ_- are the angles where the measured double differential cross section fell to half the peak value, at the angles larger and smaller than θ_0, respectively. This value is found to be always less than 0.01, while cascade calculations predict values ranging from 0.03 in C to 0.23 in Bi. This result again reinforces the description of the measurements as detecting a relatively unperturbed quasideuteron absorption.

This result has an important implication for our understanding of pion absorption in nuclei. The absorption process is described by most models: delta-hole,[2] optical potential,[1] intranuclear cascade,[3] and transport[18] calculations, as a sequence of pion scattering followed by absorption of the pion on a nucleon pair. We could expect then that the contribution to the $(\pi^+,2p)$ yield from absorption following pion scattering would be comparable to that which occurred with no scattering and the asymmetry clearly observed. This is predicted, for example, by the intranuclear cascade calculations. Except for the threshold set on the proton energy, there is no restriction in this experiment that will preclude $(\pi^+,2p)$ following pion scattering from being observed. This threshold is, however, set quite low, as mentioned earlier, and should still allow lower energy protons to be detected. The cascade calculations shown in Fig. 9 were done with the same threshold as in the experiment. These results therefore indicate that a large occurrence of two-nucleon absorption following initial-state interaction, on the energy shell, is not very likely. It appears that cascade calculations[3] and transport calculations[18] contain an overly large contribution to pion absorption from such processes. We may still have contributions from interactions where the pion was scattered near 0° before absorption because it will then keep the original opening angle. It is a question whether such scattering should be considered an initial-state interaction since, due to Pauli blocking, such events will not be related to a significant momentum transfer. We also will have to understand, then, why absorption can occur after small angle scattering but not after large angle scattering (which would appear as an asymmetry, as discussed above). If the pion scatters off the energy shell before being ab-

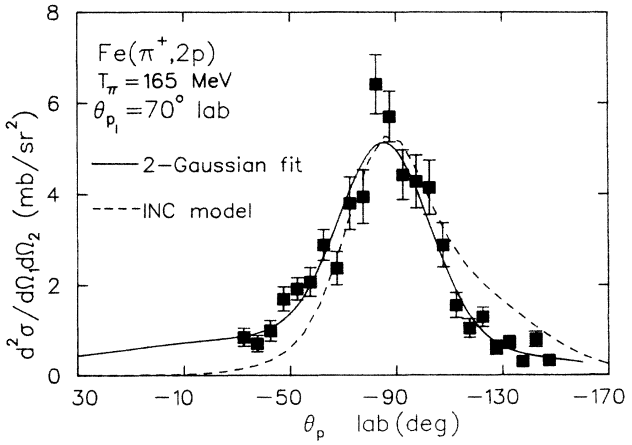


FIG. 9. The p-p angular correlation for the Fe$(\pi^+,2p)$ reaction for $\theta_{p_1}=70°$ at 165 MeV. The solid curve is the result of a two-Gaussian fit to the data; the dashed curve is a result of the INC model normalized to the amplitude of the Gaussian fit.

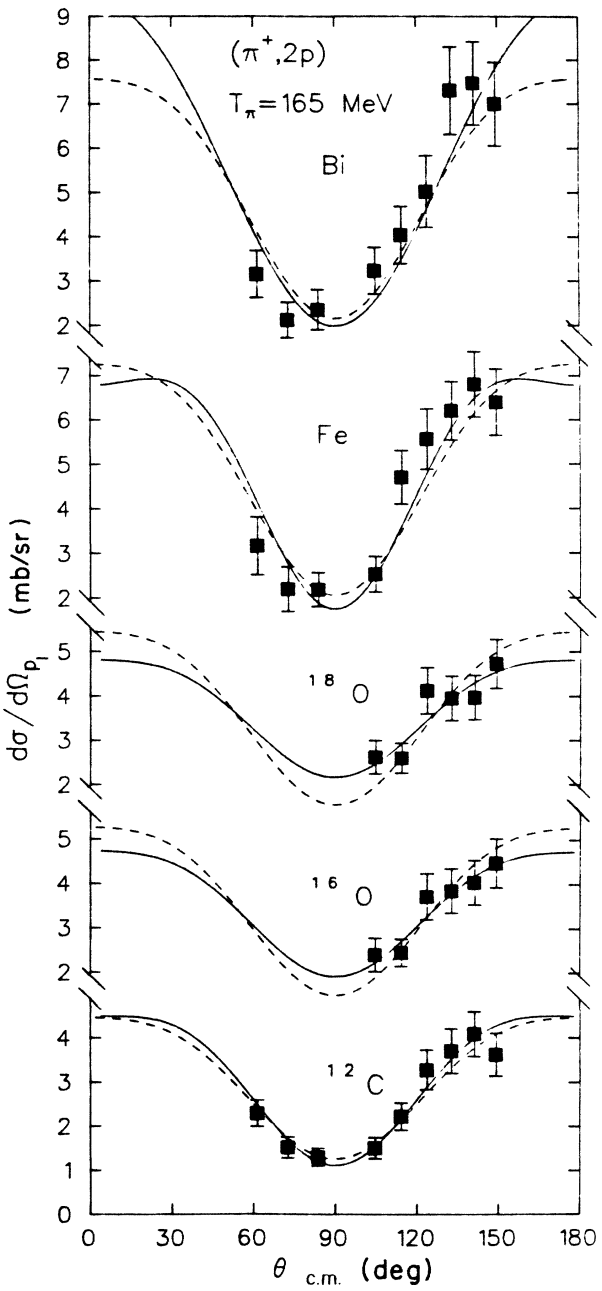


FIG. 10. The differential cross sections of the quasideuteron $(\pi^+,2p)$ reaction for C, ^{16}O, ^{18}O, Fe, and Bi at 165 MeV. The data are presented in the center-of-mass system of the $\pi^+d\rightarrow pp$ reaction. The solid curves are results of a Legendre-polynomial fits to the data. The dashed curves represent the angular distribution for the $\pi^+d\rightarrow pp$ reaction normalized to the data by the factor D_{eff} (see text).

sorbed, it will not necessarily cause an asymmetry or a shift in the angular correlation. It is a controversial question, however, whether such a process may be considered a multistep process or whether it is a genuine mode of absorption on three nucleons.

2. *Angular distributions*

In order to determine the contribution to the total absorption cross section[25] from the "quasideuteron" absorption mechanism, we integrated the area under the two-dimensional narrow Gaussian in the angular correlation. We present the resulting differential cross sections in Table II and display them as a function of $\tilde{\theta}_{p_1}$ for 165 MeV incident pions in Fig. 10 and for 245 MeV incident pions in Fig. 11. $\tilde{\theta}_{p_1}$ is the telescope's angle transformed to the center-of-mass system of the $\pi^+ d \rightarrow pp$ reaction. This transformation reflects the underlying assumption of absorption on a p-n pair, with the rest of the nucleus acting as a spectator. The solid curves in Figs. 10 and 11 represent a fit of Legendre polynomials $\sum_{k=0}^{4} A_k P_k(\cos\theta)$ to the data, with only even values of k allowed. Since most of the data were taken for angles greater than 90°, attempts to extract odd values of k would not be justified. The resulting coefficients of the fit are listed in Table III. The dashed curves in Figs. 10 and 11 represent the angular distribution for the $\pi^+ d \rightarrow pp$ reaction, normalized to

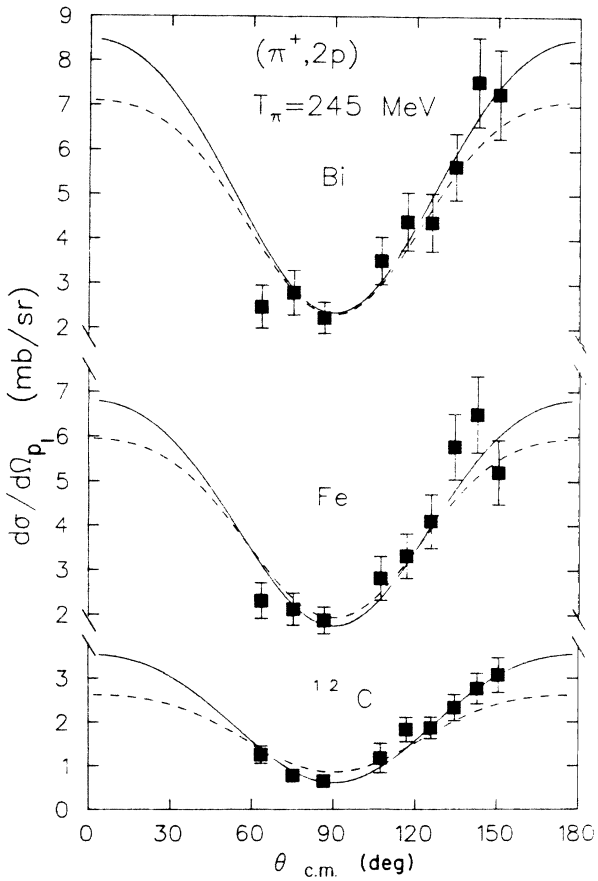


FIG. 11. The same as Fig. 10 for C, Fe, and Bi at 245 MeV.

TABLE III. D_{eff}, the coefficients from the Legendre polynomial fit to the angular distribution, the ratios between these coefficients and D_{eff}, the total quasideuteron cross section $\sigma(\pi^+,2p)$ qd, the total cross section $\sigma(\pi^+,2p)$ after final-state interaction (FSI) correction, and the ratios between these cross sections and the total absorption cross section.

Nucleus	D_{eff}	A_0 (mb/sr)	A_2 (mb/sr)	A_4 (mb/sr)	A_0/D_{eff} (mb/sr)	A_2/D_{eff} (mb/sr)	$\sigma(\pi^+,2p)^a$ qd (mb)	$\sigma_{2N}^{b,a}$ (mb)	$\sigma_{qd}/\sigma_{abs}^{c}$ (%)	$\sigma_{2N}/\sigma_{abs}^{c}$ (%)	σ_{abs}^{c} (mb)
T_π=165 MeV											
d		1.80±0.08	1.60±0.17	−0.37±0.08			11.3 ±0.5				
^{12}C	1.47±0.14	2.69±0.21	2.58±0.73	−0.79±0.71	1.83±0.20	1.76±0.50	16.93±1.34	54.67±4.54	8.7±1.8	28±6	194±36
^{16}O	1.74±0.22	3.16±0.23	2.10±0.58	−0.53±1.01	1.82±0.26	1.21±0.37	19.87±1.46	66.16±5.00	9.2±2.2	30±7	215±48
^{18}O	1.80±0.25	3.34±0.24	1.98±0.59	−0.51±1.01	1.86±0.29	1.10±0.37	21.01±1.48	71.02±7.50	8.3±1.8	28±6	252±51
Fe	2.40±0.24	4.33±0.26	4.09±0.85	−1.40±1.00	1.80±0.2	1.70±0.04	27.20±1.63	119.43±7.90	4.7±0.8	21±4	577±87
Bi	2.50±0.26	4.67±0.30	5.14±0.95	−0.35±1.10	1.87±0.23	2.06±0.04	29.36±1.86	369.07±33.34	1.9±0.4	23±5	1585±280
T_π=245 MeV											
d		0.59±0.03	0.47±0.18	−0.10±0.05			3.8 ±0.2				
^{12}C	2.65±0.26	1.75±0.10	2.08±0.35	−0.27±0.36	0.66±0.08	0.78±0.15	11.00±0.64	36.29±2.27	11.6±4.0	38±13	95±32
Fe	6.02±0.61	3.73±0.21	3.58±0.70	−0.50±0.80	0.62±0.07	0.59±0.13	23.47±1.35	123.44±8.24	5.7±1.0	30±6	411±70
Bi	7.19±0.80	4.59±0.27	5.03±0.90	−0.70±0.95	0.64±0.08	0.70±0.15	28.87±1.71	379.00±30.39	3.4±0.7	44±9	854±66

[a]The errors are statistical only and do not include normalization uncertainty (9%) and uncertainty in choosing the function for the fit.
[b]$\sigma_{2N} \equiv f\sigma(\pi^+,2p)$: corrected for FSI. For definition of f, see Sec. III B 3.
[c]σ_{abs} from Ref. 25.

the data by a factor D_{eff}, which is also listed in Table III. Comparison of the two curves shows a great similarity, thereby providing further support to the identification of the data as quasideuteron absorption. For more quantitative comparison, we list in Table III the ratios A_0/D_{eff} and A_2/D_{eff} to be compared with the values of A_0 and A_2 for the $\pi^+ d \rightarrow pp$ reaction. Again, the similarity is evident. It is interesting to note that the data for most nuclei tend to show a somewhat stronger anisotropy than for the deuteron, although they are the same within errors. Because of the large errors in determining A_4 (due to lack of data at extreme angles), we do not compare this coefficient in the table.

In Fig. 12 we show two normalization factors for ^{12}C. One is D_{eff}, the ratio between the "quasideuteron" cross section and that of the free $\pi^+ d \rightarrow pp$ reaction, which may be regarded as the effective number of quasideuterons participating in the process. The second is N_{eff}, representing the effective number of nucleons participating in pion "quasifree" scattering.[26] Although the definition of D_{eff} may not be entirely analogous to that of N_{eff}, it is interesting to note that both factors vary with broadening energy in a very similar way. This suggests a probably common origin, namely the formation of a Δ at the nuclear surface. The lower values for 165 MeV reflect the shorter mean free path for the pion at the peak of the (3,3) resonance. The value of D_{eff} at 65 MeV is taken from elsewhere.[8,27] In Fig. 13 we display the relative contribution of the quasideuteron absorption to the total absorption cross section at 165 MeV as a function of A (present work and Refs. 11 and 15). We also display in Fig. 13 the relative contribution of absorption on two nucleons to the total absorption cross section for stopped pions (Ref. 7).

3. *Final-state interaction and rescattering effects*

The total cross sections for the "quasideuteron" absorption do not account for losses due to final-state interactions of the two outgoing protons. These losses should be estimated in order to determine the contribution of the absorption on a nucleon pair to the total absorption cross

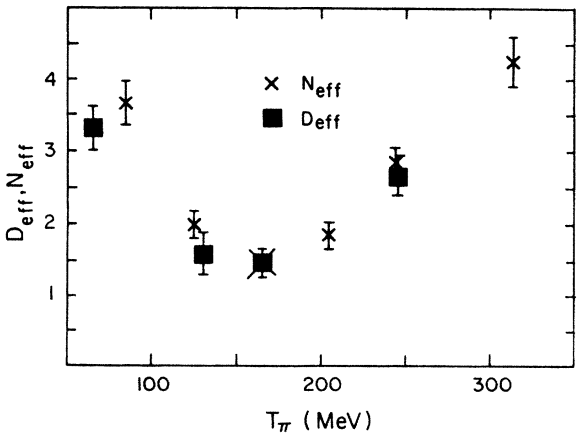


FIG. 12. D_{eff} (squares) and N_{eff} (crosses from Ref. 25) for ^{12}C as a function of the incident energy. (D_{eff} at 130 MeV is calculated from Ref. 1.)

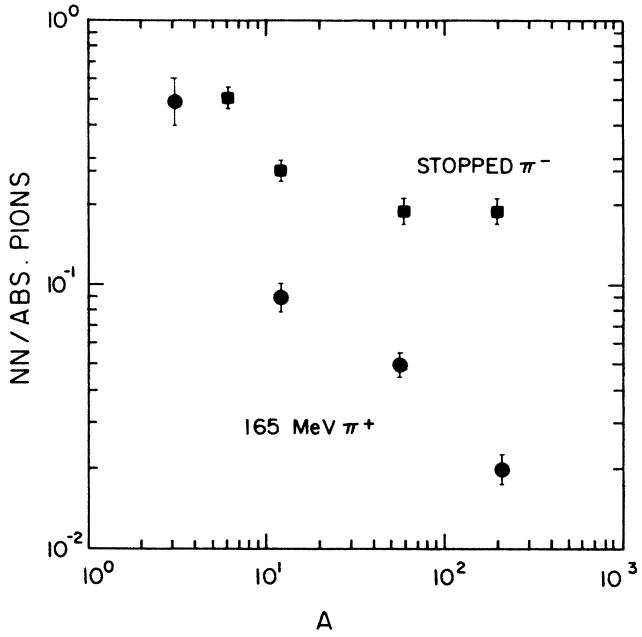


FIG. 13. The contribution of quasideuteron absorption to the total absorption rate as a function of A at 165 MeV. (Present work and Refs. 11 and 15, and for stopped pions, Ref. 7.)

section. We calculated these losses using an intranuclear cascade model. The principal features of the intranuclear cascade code (INC), and the version which was used in the present work, were described in great detail by Fraenkel *et al.*[3] We did not attempt to calculate the absolute cross section of the observed reaction by using the INC model. Instead we calculated the ratio between (a) the cross section for the $(\pi^+,2p)$ process where the pion interacts with only two nucleons before being absorbed (the outgoing protons do not undergo any further interaction with the residual nucleus or with each other, emerging with energies above the cut set in the analysis of the experimental data), and (b) the total absorption cross section for a process where the incoming pion interacts with only two nucleons before being absorbed but with no restrictions on the outgoing products which may undergo a final-state interaction. This ratio is therefore insensitive to the way the INC model treats the pion-nucleus interaction and depends only on the way it deals with nucleon final-state interaction.

The result of our calculation in the INC model is, therefore, the factor

$$f=\frac{\pi^+ + N \rightarrow \Delta;\ \Delta + N \rightarrow \text{anything out except pions}}{\pi^+ + N \rightarrow \Delta;\ \Delta + N \rightarrow 2p \text{ (no final state interaction)}} .$$

The quantity f is the factor by which we have to multiply the measured "quasideuteron" cross sections in order to account for the losses from final-state interaction. By applying this correction we obtain the contribution to the total true absorption cross section from the absorption of the pion on a nucleon pair. In Table III we present the corrected two-nucleon absorption cross sections and their

contribution to the total absorption cross sections from Ref. 25. We should note that these correction factors may be overestimated since coincidence (π,πp) experiments were found to yield more than half of the yield of (π,π') single-arm measurements,[28] and the pion mean free path must be shorter than that of a high energy proton.

C. (π^+,2p)—Conclusions

By integrating the angular distributions of Figs. 10 and 11, we obtain the total cross section for "quasideuteron" absorption. (Note that the present data and those of Ref. 23 are normalized in such a way that $\sigma = \pi \int d\sigma/d\Omega\, d(\cos\tilde{\theta})$. The results are listed in Table III, as a function of A and the incident energy, together with the total absorption cross sections.[25]

We can summarize the discussion of the (π^+,2p) reaction by the following conclusions.

(1) The identification of the narrow Gaussian in the angular correlation with a direct unperturbed absorption on a "quasideuteron" is supported and justified by four observations. (i) The peak position follows the πd→pp kinematics. (ii) The width is consistent with momentum effects of a quasifree absorption mode. (iii) The symmetry of the angular correlation around the peak indicates a process relatively free from initial-state interaction. (iv) The angular distribution of the integrated peak has a shape similar to that for the πd→pp reaction.

(2) By calculating the losses from final-state interaction using intranuclear cascade calculations, we find that the contribution to the total absorption cross section from a two-nucleon mechanism is at most between 30% and 44%. The rest of the pion absorption cross section at the above energies should be attributed to more complicated mechanisms.

(3) The energy dependence of D_{eff} as defined above reflects the variation with energy of the mean free path of the pion interacting with a nucleus. This interaction takes place mainly on the nuclear surface at the peak of the (3,3) resonance; it may involve more of the nuclear interior for incident energies far from the resonance.

The conclusion that quasideuteron absorption does not dominate the total absorption cross section raises the question of where the rest of this cross section is coming from. Several theoretical calculations propose that the pion may scatter several times before it is absorbed. In another language, that Δ's are formed, propagate, and decay several times before absorption. Since these theories[2,3] envisage such scatterings, it is conceivable that the angular correlation is smeared out after several scatterings. However, as discussed in subsection B 1, we should be able to observe contributions from absorption following one scattering as an asymmetry in the angular correlation. The contribution from such a process should be, according to these theories, comparable to that from unperturbed absorption. The failure to observe this asymmetry indicates that either this process is weak and does not account for all the missing strength, or that there must be a much larger number of scatterings such that they are all smeared into the broad Gaussian and no asymmetry due to single scattering before absorption is observed. The mechanism of double Δ excitation proposed by Brown *et al.*[29] could explain these observations if it exists in the right strength. However, so far no direct evidence for a role of such a mechanism was observed. The question remains, for the time being, open.

IV. THE ($\pi^{\pm}$,pn) REACTIONS

For the study of the ($\pi^{\pm}$,pn) reactions, angular correlations were measured for proton angles of 120°, 130°, and 140°. For each such detection angle, coincident neutrons in the detector array were detected over a horizontal angular range of about 70° for the (π^-,pn) reaction and 40° for the (π^+,pn) reaction. The vertical detection range of the neutrons was $-20° < \phi < +20°$ for both reactions. For every proton detection angle a p-n angular correlation was produced by integrating over the energies of the outgoing

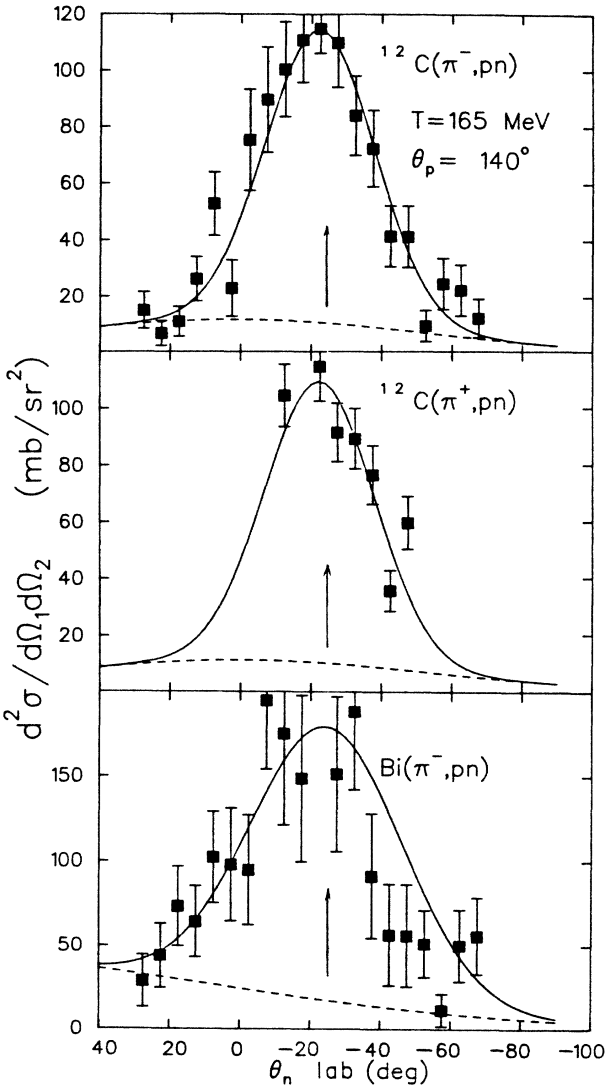


FIG. 14. Slices of the angular correlations along the reaction plane with a vertical width of ±7.5° for the ^{12}C($\pi^{\pm}$,pn) and Bi(π^-,pn) reactions at 165 MeV. The curves are the fits as described in the text.

TABLE IV. The narrow Gaussian parameters for the $(\pi^{\pm},pn)$ angular correlations. For the (π^{-},pn) reaction the peak angle was taken to be the same as obtained for the $(\pi^{+},2p)$ angular correlation (see Table II). For the (π^{+},pn) reaction both the peak angle and the standard deviation were taken to be the same as those for the (π^{-},pn) reaction. The integration over θ_n, namely, the differential cross section, is presented with the statistical error only. We also present the ratios $(\pi^{\pm},pn)/(\pi^{+},2p)$ and the ratio between the standard deviations of the $(\pi^{\pm},pn)$ and $(\pi^{+},2p)$ angular correlations.

		(π^{-},pn), narrow Gaussian parameters			(π^{+},pn)[a]	$d\sigma/d\Omega_p$ (π^{-},pn)	$d\sigma/d\Omega_p$ (π^{+},pn)			Stand dev. (π^{-},pn) / Stand. Dev. $(\pi^{+},2p)$
T		Proton angle	Amplitude	Peak angle	Stand. dev.	Amplitude	lab	lab			
(MeV)	Nucleus	(deg)	(μb/sr^2)	(deg)	(deg)	(μb/sr^2)	(μb/sr)	(μb/sr)	R_-[b]	R_+[c]	
165	^{12}C	120	76.7	37.2	16.8	90.4	41.6±6.8	49.0±13.2	33.0±6.5	28.0±8.5	1.27
		130	124.2	31.3	14.8	97.4	52.3±9.5	41.1±12.9	27.0±6.0	34.0±11.5	1.20
		140	103.5	23.3	15.4	99.0	47.8±4.6	45.7±10.3	24.0±5.0	25.5±7.0	1.26
165	^{16}O	120	90.5	36.3	17.0	87.2	50.2±8.0	48.4±9.1	28.0±6.0	29.0±7.0	1.37
		130	134.3	30.3	15.7	110.3	63.6±8.2	52.2±10.0	22.0±4.5	26.5±6.0	1.33
		140	109.4	23.4	17.4	106.1	63.2±10.6	61.3±10.6	23.0±3.5	23.6±5.0	1.45
165	^{18}O	120	83.1	36.1	17.0	97.4	46.1±5.1	54.0±5.0	32.0±5.5	27.0±4.5	1.32
		130	121.8	30.3	15.2	108.1	53.7±6.0	47.7±6.5	25.0±4.5	28.5±5.5	1.24
		140	90.2	22.7	17.2	105.2	51.2±6.0	59.7±8.0	30.0±5.0	25.5±5.0	1.40
165	Bi	120	154.1	38.7	21.6		137.1±28.4		19.5±5.0		1.20
		130	175.8	31.8	20.5		141.0±20.0		18.0±3.5		1.28
		140	161.8	25.5	21.6		144.0±24.5		16.0±3.5		1.44
245	^{12}C	120	94.7	34.7	13.7	70.7	34.1±5.7	25.2±5.5	24.0±5.0		1.16
		130	100.1	28.4	14.7	67.3	41.3±7.2	27.8±6.5	21.0±4.5		1.20
		140	50.7	21.3	15.7	68.0	24.0±4.5	32.1±5.1	37.0±8.0		1.21
245	Bi	120	117.1	35.1	19.3	144.4	83.2±16.5	102.6±26.0	23.0±5.0		1.20
		130	169.7	27.7	21.4	225.5	148.6±26.5	196.8±41.5	16.0±4.0		1.20
		140	102.5	20.3	21.8	134.1	93.4±16.0	122.1±36.0	23.0±5		1.29

[a]The peak angle and standard deviation for (π^{+},pn) are the same as for (π^{-},pn) (see text).

[b]$R_- = (d\sigma/d\Omega)_{\pi^+,2p}/[2(d\sigma/d\Omega)_{\pi^-,pn}]$.

[c]$R_+ = (d\sigma/d\Omega)_{\pi^+,2p}/2[(d\sigma/d\Omega)_{\pi^+,pn}]$.

nucleons above the same cutoff used for the (π^+,2p) reaction, as described in Sec. III A. Figure 14 displays a slice of the angular correlation along the reaction plane with a vertical width of $\Delta\phi = \pm 7.5°$, for the ^{12}C($\pi^{\pm}$,pn) and Bi(π^-,pn) reactions at an incident energy of 165 MeV. A pronounced peak is observed in the angular correlation for the (π^-,pn) reaction at the angle corresponding to the kinematic condition of the $\pi^+ d \rightarrow pp$ reaction. The data in the angular correlation of the (π^+,pn) reaction cover a smaller part of the two-body kinematical region. The errors shown in the figures contain statistical and angle-dependent systematic uncertainties. There is an additional overall normalization uncertainty of $\sim 18\%$ coming from uncertainties in secondary reactions, target correction flux, and solid angles, (10%), and from uncertainty in the determination of the neutron efficiency ($\sim 15\%$).

To obtain the two-body contribution to the (π,pn) angular correlations, we fitted the data to two Gaussian functions as described in the discussion of the (π^+,2p) case. For the (π^-,pn) reaction we set the peak positions of the narrow Gaussian to the values obtained from the corresponding (π^+,2p) angular correlation for the same target at the same energy and angle. This presetting of the positions was aimed to avoid the inclusion of events from the (π^-,π^-n) reaction. Since $\sigma(\pi^-,\pi^-\text{n})/\sigma(\pi^-,\text{pn}) > 100$, any leak of neutrons from the (π^-,π^-n) reaction (due to misidentifications of the scattered pion) would have a significant effect on the (π^-,pn) angular correlations. (The angular correlations of the two reactions are separated by 10°—15°.) A few events from the (π^-,π^-n) reaction appear ocassionally as a shoulder or high background in the small angle side of some of the angular correlations. The other parameters of the fit to the (π^-,pn) angular correlations were left free.

For the angular correlations of the (π^+,pn) reaction we used the peak positions and the widths obtained from the fit of the (π^-,pn) data. We also kept the ratio between the amplitude of the narrow Gaussian and the broad one and let only the absolute magnitude be free. This procedure was necessary because the angular correlations of the (π^+,pn) reactions covered a more limited angular range.

The solid curves in Fig. 14 represent the sum of the resulting two Gaussian functions. The dashed curves are the broad Gaussian backgrounds alone. By integrating over the narrow Gaussian, we obtained the contributions from the absorption of π^- on p-p pairs and of π^+ on n-n pairs. In Table IV we present the parameters of the narrow Gaussians obtained by the above fitting procedures and integrations over these Gaussians yielding the differential cross sections.

Also listed are the ratios

$$\frac{1}{2}\left[\frac{d\sigma}{d\Omega}(\pi^+,2\text{p}) \Big/ \frac{d\sigma}{d\Omega}(\pi^{\pm},\text{pn})\right].$$

The factor $\frac{1}{2}$ comes from the fact that in the ($\pi^{\pm}$,2p) reaction both protons can be detected by both counters. Table IV also contains ratios of the widths of the narrow Gaussians in the (π,2p) and (π,pn) reactions. These ratios show that for the (π,pn) reactions the width of the angular correlation is about 20% larger than for (π^+,2p). This may reflect a larger internal momentum of the $T=1$ (p-p or n-n) absorbing pair, as compared with the $T=0$ (p-n) pair. We should note, however, that since the (π,pn) reactions are so weak, their angular correlation may be affected by many secondary processes, such as final-state interaction of the out-going nucleons, which may affect their shape. This point is further discussed later in this section.

The cross-section ratios presented in Table IV are large and similar to the ratios observed in ^{3}He.[16,17] The large ratios observed in ^{3}He were interpreted[16] to result from a suppression of the absorption process on a $^1S_0$ $T=1$ pair, since an intermediate state with a ΔN in a relative S state is not allowed. This state is responsible for the large absorption cross section on the deuteron. On nuclei heavier than He, an absorbing proton or neutron pair does not have to be in a $^1S_0$ state and then an intermediate ΔN system in a relative S state could be formed. The fact that the cross-section ratios are still so large indicates that absorption on such pairs is unfavored by the dynamics of the absorption mechanism. Comparison of the (π^+,pp) and ($\pi^{\pm}$,pn) reactions on ^{16}O and ^{18}O reveals interesting isotopic effects which were discussed elsewhere.[14]

We investigated the possibility that part of the (π,pn) yield originates from the much stronger ($\pi^{\pm}$,2p) or (π^-,2n) reactions followed by nucleon charge exchange. Calculations using intranuclear cascade model[3] showed such yield, but its angular correlation was broad and hence mostly removed as part of the broad Gaussian. Attempts to observe the (π^-,pp) yield, which could originate from such processes (the probability is squared, but proton detection efficiency is 100%), yielded only upper limits, indicating a small probability. In a recent work with stopped π^- in ^{6}Li a 0.26% probability for the forward nucleon charge exchange process was deduced from (π^-,2p) yield.[30] This would mean that less than 10% of the (π,pn) narrow Gaussian yield may come from such processes. Supporting this conclusion is also the observation that the cross-section ratio does not vary strongly with the nuclear mass; a large nucleon charge exchange component should manifest itself as a strong A dependence of the (π,pn) cross section.

We finally note that these cross-section ratios were also measured at lower energies: 65 MeV (Refs. 8 and 27) and for stopped π (Ref. 31) [where (π^-,2n)/(π^-pn) rate ratios were measured]. The measured ratio for C gradually decreases from about 25 at the resonance region to about 5 at 65 MeV and down to 2.5 for stopped pions.

In conclusion, we presented results of studies of the (π^+,2p) and ($\pi^{\pm}$,pn) reactions where the direct two-nucleon absorption component is identified. For the (π^+,2p) reaction this component accounts for only about 10% of the absorption cross section for carbon, down to about 2% for bismuth. With corrections for final-state interaction of the out-going protons, it amounts to at most 40%. The results also indicate that a significant contribution from quasideuteron absorption following on-shell scattering of the pion is not likely. The direct absorption on $T=1$ nucleon pairs is about 4% of that on $T=0$

pairs, similar to the ratio observed for the elementary process.

ACKNOWLEDGMENTS

We thank Professor C. Joseph for allowing us to use the detector array and H. Ulrich for the neutron efficiency calculation code. Illuminating discussions with Dr. F. Lenz, Dr. J. Schiffer, and Dr. E. Osset are gratefully acknowledged. We owe special thanks to Professor Z. Fraenkel for helping us in using the INC code and advising us about the interpretation of its results. The Tel-Aviv University group is grateful for the warm hospitality of the Schweizerisches Institut für Nuklearforschung. This work was supported in part by the Israeli Commission for Basic Research and by the Swiss Institute for Nuclear Research.

---

*Present address: TRIUMF, Vancouver, British Columbia, Canada V6T 2A3.

†Permanent address: California Institute of Technology, Pasadena, CA 91125.

[1]K. Masutani and K. Yazaki, Phys. Lett. **104B**, 1 (1981).

[2]K. Yazaki, in Proceedings of the Symposium on Delta-Nucleus Dynamics, edited by T. S. H. Lee *et al.*, Argonne National Laboratory Report No. ANL-PHY-83-1, May 1983 (unpublished).

[3]Z. Fraenkel, E. Piasetzky, and G. Kälbermann, Phys. Rev. C **26**, 1618 (1982).

[4]J. Favier *et al.*, Nucl. Phys. **A169**, 540 (1971).

[5]E. D. Arthur *et al.*, Phys. Rev. C **11**, 332 (1975).

[6]B. Bassalleck *et al.*, Nucl. Phys. **A343**, 365 (1980).

[7]P. Heusi *et al.*, Nucl. Phys. **A407**, 429 (1983).

[8]H. Yokota *et al.*, Phys. Rev. Lett. **51**, 1531 (1983); K. Nakayama *et al.*, Phys. Rev. C **33**, 1002 (1986).

[9]M. Ericson and T. E. O. Ericson, Ann. Phys. (Leipzig) **36**, 323 (1966).

[10]See, for example, Y. Horikawa, M. Thies, and F. Lenz, Nucl. Phys. **A345**, 386 (1980).

[11]E. Bellotti *et al.*, Nuovo Cimento **18A**, 75 (1973).

[12]A. Altman *et al.*, Phys. Rev. Lett. **50**, 1187 (1983).

[13]R. D. McKeown *et al.*, Phys. Rev. C **24**, 211 (1981); R. D. McKeown *et al.*, Phys. Rev. Lett. **44**, 1033 (1980); J. P. Schiffer, Commun. Nucl. Part. Phys. **10**, 243 (1981); J. W. Negele and K. Yazaki, Phys. Rev. Lett. **47**, 71 (1981); J. P. Schiffer, Nucl. Phys. **A335**, 339 (1980).

[14]A. Altman *et al.*, Phys. Lett. **144B**, 337 (1984); see also D. Ashery, in Proceedings of the Symposium on Delta-Nucleus Dynamics, Ref. 2, p. 23.

[15]D. Ashery *et al.*, in Proceedings of the PANIC Conference, Heidelberg, 1984, abstract E20; see also D. Ashery *et al.*, Phys. Rev. Lett. **47**, 895 (1981).

[16]G. Backenstoss *et al.*, Phys. Lett. **137B**, 329 (1984); G. Backenstoss *et al.*, in Proceedings of the PANIC Conference, Heidelberg, 1984, abstracts E15 and E16.

[17]M. Moinester *et al.*, Phys. Rev. Lett. **52**, 1203 (1984); A. Altman *et al.*, in Proceedings of the PANIC Conference, Heidelberg, 1984, abstracts E17—E19; K. Aniol *et al.*, Phys. Rev. C **33**, 1714 (1986).

[18]V. Girija and D. S. Koltun, Phys. Rev. Lett. **52**, 1397 (1984).

[19]R. J. Kurz, University of California Report No. UCRL-1139, Mar. 1964/Feb. 1965 (unpublished); see also S. A. Elbakr *et al.*, Nucl. Instrum. Methods **115**, 115 (1974).

[20]D. Gotta, J. Miers, and H. Ulrich, private communication,

[21]Guex Le Lan Huong, Ph.D. thesis No. 245, Ecole Polytechnique Federale dè Lausanne, 1976.

[22]P. J. Bussy *et al.*, Nucl. Phys. **B58**, 363 (1973).

[23]C. Richard-Serre *et al.*, Nucl. Phys. **B20**, 413 (1970); M. G. Albrow *et al.*, Phys. Lett. **34B**, 337 (1971); H. Nann *et al.*, *ibid.* **88B**, 259 (1979).

[24]B. G. Ritchie *et al.*, Phys. Rev. C **30**, 969 (1984).

[25]D. Ashery *et al.*, Phys. Rev. C **23**, 2173 (1981).

[26]I. Navon *et al.*, Phys. Rev. C **22**, 717 (1980).

[27]H. W. Roser *et al.*, in Proceedings of the PANIC Conference, Heidelberg, 1984, abstract F12.

[28]E. Piasetzky *et al.*, Phys. Rev. Lett. **46**, 1271 (1981); Phys. Rev. C **25**, 2687 (1982).

[29]G. E. Brown *et al.*, Phys. Lett. **118B**, 39 (1982); see also E. Oset *et al.*, in Proceedings of the PANIC Conference, Heidelberg, 1984, abstract E25.

[30]M. Dorr *et al.*, Nucl. Phys. **A445**, 557 (1985).

[31]H. P. Isaak *et al.*, Helv. Phys. Acta **55**, 477 (1982).